2020 IEEE/RSJ International Conference on Intelligent Robots and Systems (IROS)
October 25-29, 2020, Las Vegas, NV, USA (Virtual)

Designing A Dummy Skin by Evaluating Contacts between A Human Hand and A Robot End Tip

Yumena Iki*, Yoji Yamada*, Yasuhiro Akiyama*, Shogo Okamoto*, and Jian Liu*

Abstract— **Many manufacturing industries have a high demand for the construction of collaborative operation systems using industrial robots. Although there is a preexisting set of safety verification data in ISO/TS 15066 for collaborative operations, there is no established testing method for safety validation. To establish a testing method, it is effective to use a dummy that has mechanical properties similar to those of a human. However, there is no parametric study that exists for designing a dummy that represents the static and dynamic mechanical properties and the nonlinearity of the static mechanical properties. In this study, static and dynamic experiments were conducted to obtain the mechanical stiffness of human subjects and the contact force transitions during the dynamic contact between a robot system and a human. Subsequently, the same experiment was conducted using the proposed dummy. The biofidelity of the dummy was examined by comparing the parameters of a viscoelastic model. This study contributes to increasing the safety of collaborative operations by developing a dummy that can be used for risk assessments in collaborative operations.**

I. Introduction

Recently, there is a high demand for industrial robots that can be used to improve the productivity of collaborative operations. In these situations, robot systems and humans share the same workspace, resulting in various technical questions, including whether contact between them is acceptable. To address this problem, in the field of robotics, Suita and Yamada et al. discussed a method to achieve a safe human-robot coexistence by proposing that human somatic pain must be the criteria for acceptability [1], [2], [3]. In relation with pain, Saito and Ikeda proposed the force and deformation tolerance limits of the sense of pain for the safety design of human-robot collaborative operations from static measurement [4]. Povse et al. determined the correlation between the intensity of subject pain perceived during human-robot collision and the impact energy density, which is a function of the values of impact force, contact surface area, and displacement [5]. These studies were based on pain tolerance. Today, ISO/TS 15066 is an internationally accepted guideline for collaborative operation. It clarifies appropriate procedures for the limit of speed values that maintain force and pressure values under the pain sensitivity threshold. The biomechanical limit force and pressure values for the pain onset levels for the transient and quasi-static events were proposed in the worst-case scenario. These worst cases indicate when a robot system may clamp or pin a human body [6]. However, as mentioned by Pilz, ISO/TS 15066 provides insufficient guidance on how the test must be setup and the procedure to follow [7]. Therefore, it is necessary to establish a testing method for safety validation.

To establish a testing method, it is effective to use a dummy because there are various types of industrial robots with differing types of contact, pressure and force that must be tracked on the human side in a human-robot system interaction. A dummy can be attributed with mechanical properties similar to those of a human and be equipped with sensors. While cases where human subjects are impacted must be carefully considered from an ethical viewpoint, the dummy may be provided with an impact that corresponds to its biomechanical limits to simulate this interaction.

There have been numerous studies that investigate human mechanical properties in a dummy. The Code of Federal Regulation provides the force-deflection curve when designing a dummy for highway traffic safety, which can also be used for such a collaborative operation between robot systems and humans that is necessary to consider a lower level of impact, as mentioned by Haddadin et al. [8], [9]. Panasonic Corporation developed a full arm dummy for a human-inspired pain-sensing system by focusing on the pain-free interaction between personal care robots and humans. They verified the biofidelity of their human arm dummy through the force and displacement curve [10]. These studies express the human static mechanical properties of the human skin-like force-displacement curve while also considering the nonlinearity of the static mechanical properties. However, they do not focus on the dynamic aspect of the mechanical properties of materials, although it is crucial to consider dynamic parameters. The dynamic parameters are an indispensable consideration from the perspective of injury. Desmoulin and Anderson determined contusion tolerance according to absorbed energy [11]. Fujikawa and Sugiura et al. proposed that the peak mean contact pressure and the total transferred energy in mechanics total energy supplied to the skin of substitute animals should be considered as the dominant parameters of bruise [12], [13]. All these parameters are determined by the dynamic parameters. In collaborative operations, contact between the robot system and humans is commonly dynamic, and the peak values of the transient contact force or pressure, according to ISO/TS 15066, depends on the dynamic mechanical properties such as viscosity. GTE Industrieelektronik GmbH constructs a measuring system considering not only spring constants according to ISO/TS 15066 but also damping materials using Deutsche Gesetzliche Unfallversicherung information [14]. Povse et al. developed a human lower arm dummy that can

*All authors are with Department of Mechanical Systems Engineering, Nagoya University, Nagoya, 464-8603, Japan iki.yumena@g.mbox.nagoya-u.ac.jp

accurately replace humans from the viewpoint of impact force and impact point speed [15]. However, their system is short of quantitative parametric information.

Many studies model the static and dynamic mechanical properties by considering the viscoelasticity. Dinnar was the first to propose a viscoelastic model for human skin tissue [16]. He used two springs and two dashpots to represent the epidermis, dermis, and subcutaneous tissue. There are many viscoelastic models that represent human mechanical properties in combination with springs, dashpots, and other elements for human skin [17], [18], [19] and human organs [20], [21]. However, their objective is usually for medical applications, rather than modeling human mechanical properties of a dummy for collaborative operation.

Another method that considers the mechanical properties of humans is the finite element method in [22], [23]. However, it is difficult to apply this method to the development of a dummy, since a simple analytical model is required to confirm the validity of the selected parameters.

No parametric study exists to design a dummy representing the static mechanical properties of humans and also the dynamic mechanical properties and nonlinearity of the static mechanical properties from a holistic viewpoint. This study develops such a dummy, which can be used for risk assessment when introducing collaborative operations in the manufacturing industry, thereby contributing to increasing safe collaborative operations. First, we constructed an experimental apparatus to evaluate the static and dynamic contact between a robot end-effector and a human in a clamping situation, which is generally considered to be the worst-case to measure the stiffness of human subjects and the transition of the contact force during the impact. Subsequently, the same experiment is conducted using the developed dummy. The biofidelity of the dummy is examined by comparing the parameters of a series model each comprising a 3-element Maxwell model. The parameters are optimized by a genetic algorithm using MATLAB (with version 2019a) Simulink Model.

II. Methods/Experiment

A. Setup

Fig. 1 illustrates the experimental setup assuming the clamping situations considered to be the worst-case scenario for contact between a robot system and a human during collaborative operation. The experiment was conducted with the approval of the Ethics Committee of the Department of Engineering, Nagoya University.

Two safety devices were established to safely perform this experiment.

The first was a movable stand with a release mechanism fixing the hand of a subject, as depicted in Fig. 2. The stand was attached to a magnet with a slider. If a subject felt any discomfort, or if the force applied to him/her was higher than the attractive force of the magnet, they could avoid contact immediately by activating the release mechanism. The attractive force of the magnet was set to approximately 100 N.

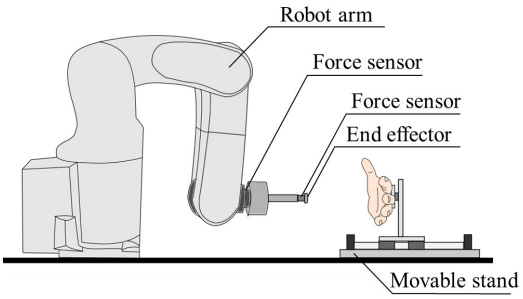

Fig. 1: Experimental setup

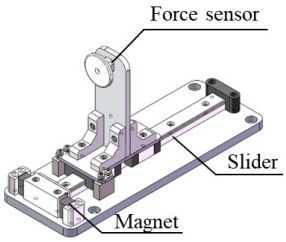

Fig. 2: Movable stand

The second was the force control system, which comprised two force sensors; one mounted at the end-effector of the robot arm, and the other attached to the impactor. The robot arm was programmed to stop the movement when the measured value from either one of the force sensors was observed erroneous or when the force applied to the subject was higher than the pre-set value. The value was set to 100 N in this experiment.

The contact surface of the impactor was 14 mm^2. A chamfer plane of 2 mm was formed on each side of the contact surface. The contact surface was chosen to be the same as that in ISO/TS 15066 for safety validation.

B. Procedure

The procedure was divided into two parts.

The first part involved a static experiment. The robot arm was moved from its original position, which was approximately 100 mm away from the contact part in the horizontal direction, as depicted in Fig. 1. It was slowly shifted towards the contact part. Three positions were determined by the static contact force, as illustrated in the next section.

The second part consisted of a dynamic experiment. The robot arm was reverted to its original position after the static experiment. It was subsequently moved to a position that was determined in the static experiment to ensure the occurrence of impact at a constant contact speed. Two modes of contact speeds were commanded, as detailed in the subsequent section.

In both experiments, the contact force was measured by the force sensors and the position and speed of the robot arm were measured by the robot system.

C. Conditions

The positions determined in the static experiment assumed the static contact force to be 5, 10, and 15 N. The maximum static contact force was set to 15 N because subjects would not experience pain below the range for static contact force. However, if the subjects noted discomfort, the experiment was stopped immediately. The contact speeds for the dynamic experiment were set at 10 and 250 mm/s, which represent quasi-static and dynamic contacts, respectively. The dynamic experiment was conducted thrice for each subject and once for a dummy under each condition.

D. Targets

Five male subjects participated in this study. The targets were three parts (forefinger pad, palm, and thenar eminence) of the human body model, as shown in Fig. 3. These contact points of the human body model were determined using ISO/TS 15066. When considering the frequency of contact, it is generally observed that contact is more likely to be made at the back of human hands. It is hazardous, however, to conduct contact experiments at the back of the hands, and we targeted the palm side of the hand as the initial focus of this study.

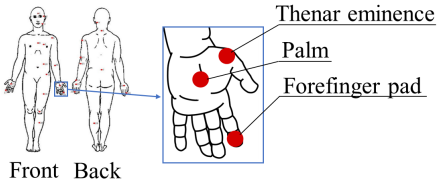

Fig. 3: Contact parts

The dummy developed in this study was composed of urethane fabricated by the Tanac Corporation, as depicted in Fig. 4. It simulates the palm of the subject. It consists of two layers with a thickness of 5, and 10 mm.

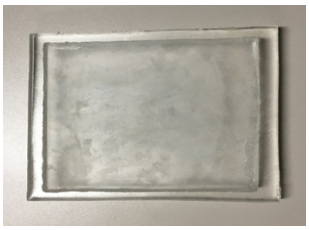

Fig. 4: Dummy skin

E. Model

Maxwell and Voigt models are the representative ones for the viscoelastic behaviors of the materials. In general, all viscoelastic behaviors of materials can be expressed by combining these models.

From the preliminary experiment, it was found that when the robot arm comes in contact a human at a high speed, there are two types of time constants: rapid relaxation just after the maximum contact force and slow relaxation later. It is considered that this phenomenon is caused by the different characteristics of human multilayered soft tissue. In this study, a series model of the simplest 3-element Maxwell model was applied to represent human multilayered soft tissue. Each 3-element Maxwell model was considered as one layer that can be expressed by one material. Fig. 5 depicts the applied series model of 3-element Maxwell model. The model determines that the stiffness is proportional to the square of its displacement expressed as $\alpha_i {x_{\alpha_i}}^2$ and $\beta_i {x_{\beta_i}}^2$ and the viscosity is constant expressed as c_i experimentally ($i = 1, 2$; number of layers). α_1 was set to be greater than α_2 for the static parameters.

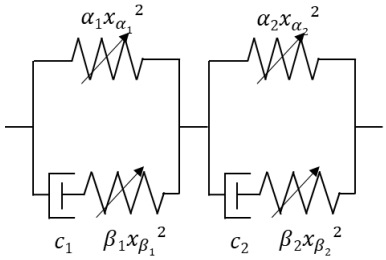

Fig. 5: Series model of a 3-element Maxwell model

F. Methods

The genetic algorithm technique with MATLAB (with version 2019a) Simulink Model was used to optimize the parameters of the applied model for the dynamic experiment based on the method described in [24]. It searches for an optimal solution that minimizes the error between the transient contact force from the experiment and the output from the Simulink Model for the speed input of the robot arm from the experiment.

III. Results

A. Static response

Fig. 6 depicts the stiffness of the palm of five subjects (black lines) and the dummy skin (red line). The displacement corresponding to 10 and 15 N static contact force falls in the individual difference ranging from 8.8-11.9 mm and 10.2-13.1 mm, respectively. This is independent of the fact that the displacement corresponding to 5 N static contact force is 0.4 mm outside the individual difference ranging from 6.6-10.0 mm, meaning that it is a little stiffer in the small displacement range. However, the stiffness of the dummy skin generally exhibits properties similar to those of the subjects.

B. Dynamic response

Fig. 7 illustrates the transient contact force of the palm of one subject (gray lines) observed thrice in the experiment and the optimized curve estimated by the genetic algorithm (red line) under each condition. The contact speed is 10 mm/s in the upper figures and 250 mm/s in the lower figures. The displacement assumes that the static contact force becomes 5, 10, and 15 N from the left figure. The

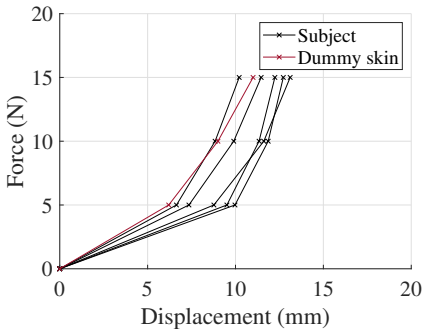

Fig. 6: Stiffness of the palm of five subjects (black lines) and the dummy skin (red line)

contact force increases nonlinearly after the contact starts, attains the maximum value when the robot arm reaches the maximum displacement, and after that, the contact force relaxation occurs. The vibratory signal variation observed in the phase of the contact force relaxation is due to the pulse of the subject.

Fig. 8 illustrates the transient contact force of the dummy skin (black line) and the optimized curve estimated by the genetic algorithm (red line) under each condition. The contact speed is 10 mm/s in the upper figures and 250 mm/s in the lower figures. The displacement assumes that the static contact force becomes 5, 10, and 15 N from the left figure, respectively. The transient contact force of the dummy skin generally shows properties similar to those of the subjects when comparison is made between Fig. 7 and Fig. 8.

Fig. 9 illustrates the maximum dynamic contact force of the palm of five subjects and the dummy skin under each condition. The bar graphs are those of the subjects, and the points in red circles are those of the dummy. The horizontal axis represents each condition (f is the static contact force and s is the contact speed.). Table I displays the mean (standard deviation) values of the subjects and the dummy. The maximum contact force becomes large when the contact speed becomes high under the same static contact force owing to viscosity. When comparing only the maximum dynamic contact force, the values of the dummy are included in the range of individual differences under all conditions.

TABLE I: The mean (standard deviation) values of the maximum dynamic contact force (N) of the subjects and the dummy

Condition		Subject	Dummy
f (N)	s (mm/s)		
5	10	8.2 ± 0.5	8.3
5	250	9.0 ± 1.0	10.1
10	10	14.8 ± 1.6	15.0
10	250	17.0 ± 1.8	17.7
15	10	21.7 ± 2.5	20.9
15	250	27.3 ± 2.6	26.1

C. Optimized parameters

Fig. 10 depicts the optimized parameters of the palm of five subjects (bar graphs) and the dummy (colored circles). The bar graph of each parameter contains all conditions regardless of static contact force and contact speed because no difference is observed depending on these conditions. Table II shows the mean (standard deviation) values of each parameters for the subjects' palms and the dummy. The differences between α_1 and α_2, β_1 and β_2, and c_1 and c_2 are distinct, showing the different characteristics of multilayered soft tissue.

TABLE II: The mean (standard deviation) values of the parameters of the subjects and the dummy

Parameter	Subject	Dummy
α_1 (N/mm^3)	0.29 ± 0.27	0.34 ± 0.19
α_2 (N/mm^3)	0.04 ± 0.03	0.06 ± 0.02
β_1 (N/mm^3)	0.68 ± 0.52	0.45 ± 0.23
β_2 (N/mm^3)	0.13 ± 0.15	0.64 ± 0.35
c_1 (N/(mm/s))	3.24± 2.67	5.10 ± 2.53
c_2 (N/(mm/s))	1.93± 2.39	0.40 ± 0.28

IV. Discussion

A. Static response

As mentioned in the previous section, the stiffness of the dummy skin is harder than those of the subjects in smaller ranges of displacement, as shown in Fig. 6. Two phases appear in the stiffness of the subjects: the slow curve in small displacement and the rapid curve in large displacement. When the displacement is small, the contact force does not increase rapidly because the dermis, which consists of water and collagen, moves. However, when the displacement reaches the limit where the dermis can no longer move easily, soft tissue, such as the epidermis, dermis, and subcutaneous tissue, is clamped by the hard tissue, such as the bone, and the contact force increases rapidly as a result. This phenomenon is pertinent only to human soft tissue.

B. Dynamic response

When focusing on the phase until arriving at the maximum dynamic contact force of the transient contact force (Fig. 11 and 12), the viscosity of the dummy is observed to be larger than that of the subjects; in particular, a convex shape can be seen under the condition that the contact speed is 250 mm/s for the dummy. It is said that the peak mean contact pressure and the total transferred energy are the dominant parameters for injury in [13]. The total transferred energy was obtained by eq.1.

$$U = \frac{1}{A}\int_0^{\delta_1} F d\delta \tag{1}$$

where A is the contact area, F is the applied contact force, δ is the displacement, and δ_1 is the maximum displacement.

The dummy we developed is quite useful from the viewpoint of safety validation for injury because the dummy

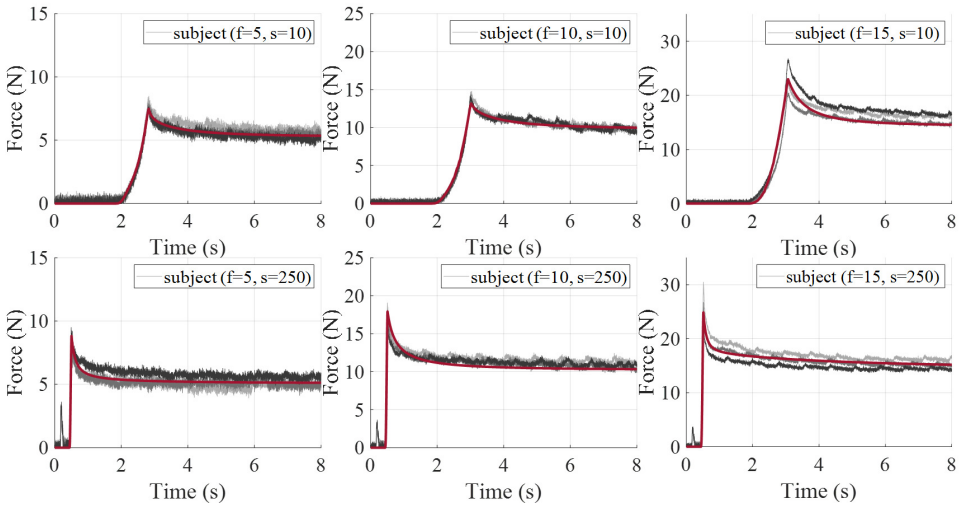

Fig. 7: Transient contact force of the palm of one subject (grey lines) and the optimized curve (red line) under each condition

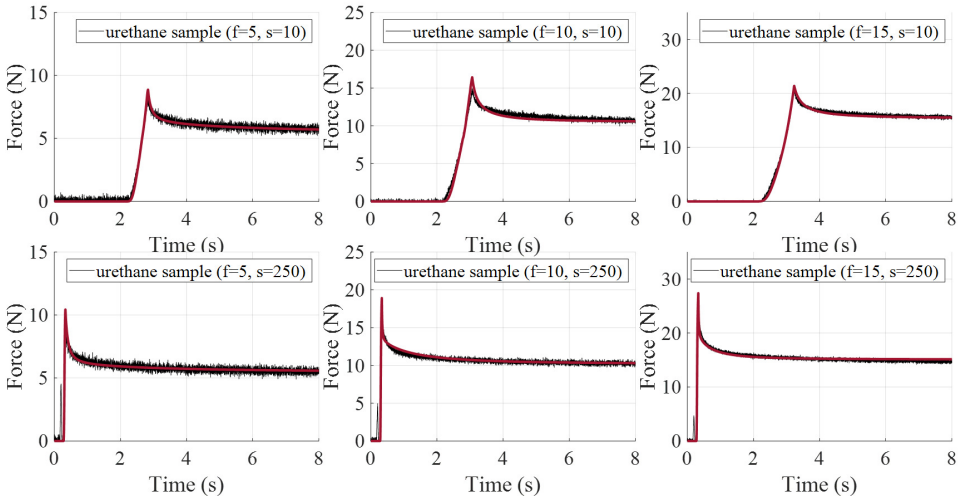

Fig. 8: Transient contact force of the dummy skin (black line) and the optimized curve (red line) under each condition

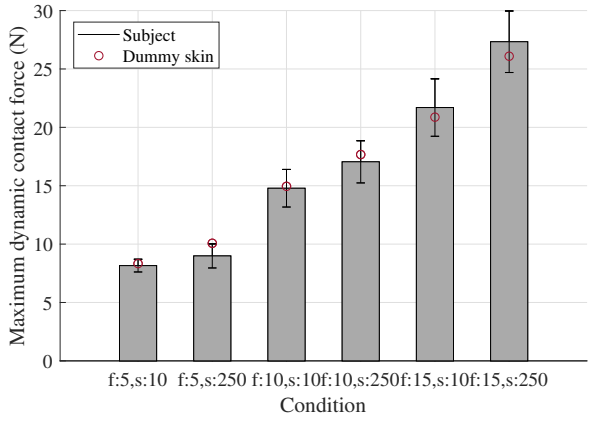

Fig. 9: Maximum dynamic contact force of the palm of five subjects (bar graphs) and the dummy (red circles) under each condition (f: static force, s: contact speed)

shows the same maximum dynamic contact force as that of the subjects (Fig. 9), while the total transferred energy (Fig. 11 and 12) is estimated to be higher than that of the subject, making criteria safer than the subject.

C. Optimized parameters

To examine the biofidelity of the dummy, Mann Whitney's U test, which is a non-parametric test, and Welch's t-test, which is one of the parametric tests, was conducted on the results of Fig. 10. Table III depicts the results of Mann Whitney's U test and Welch's t-test. The asterisks ** and *** indicate that the coefficients show statistical difference of significance at 5 and 1 percent level, respectively. The significant difference cannot be seen except for α_2 by Mann Whitney's U test and β_2 by both tests. The difference in α_2 is caused by the difference in stiffness, as mentioned above. The difference in β_2 is caused by that of the viscoelasticity in the experiment where the impact profile arrives at the maximum dynamic contact force. As mentioned above, we can conclude that the biofidelity of the dummy is considerably

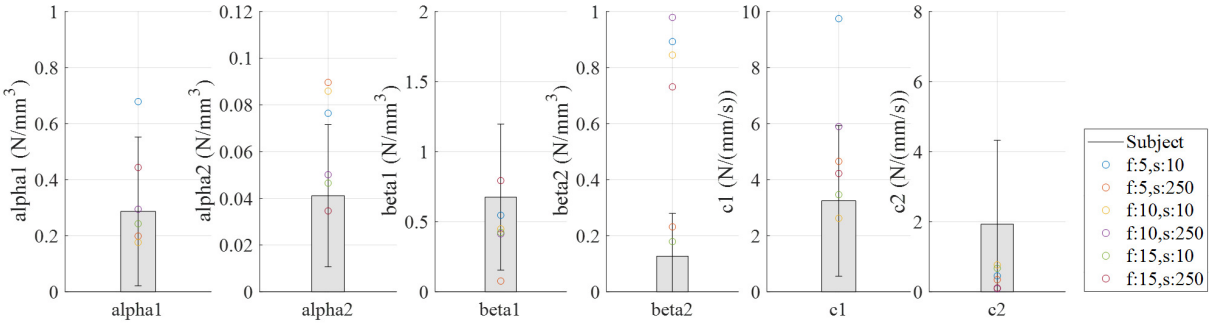

Fig. 10: Optimized parameters of the palm of five subjects (bar graphs) and the dummy (colored circles) (not to scale between each parameter)

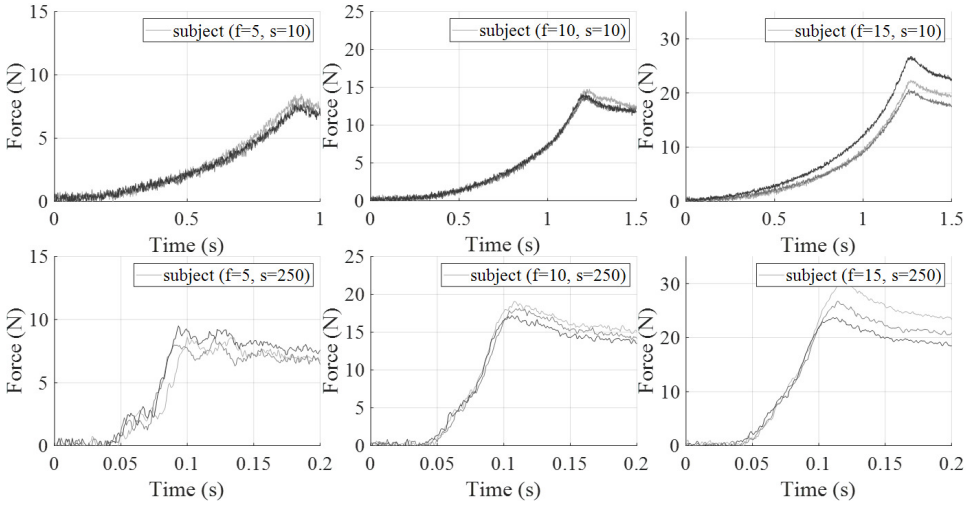

Fig. 11: Transient contact force of the palm of one subject until it arrives at the maximum dynamic contact force under each condition

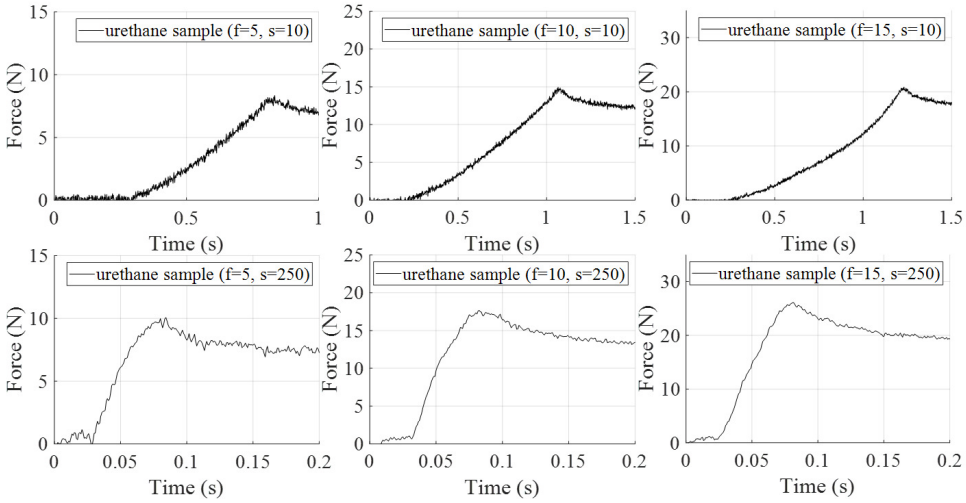

Fig. 12: Transient contact force of the dummy skin until it arrives at the maximum dynamic contact force under each condition

high.

TABLE III: The results of Mann Whitney's U test and Welch's t-test

parameter	Mann Whitney's U test	Welch's t-test
α_1	0.18	0.65
α_2	**	0.09
β_1	0.46	0.31
β_2	***	***
c_1	0.18	0.13
c_2	0.16	0.13
		$n_{subject}$ = 30
		n_{dummy} = 6

V. Conclusion and future work

In this study, we developed a dummy skin to mimic a human hand palm with considerably high biofidelity. The experimental setup was constructed assuming clamping situations that represented the worst-case scenarios for contact between robot systems and humans in collaborative operation. Static and dynamic contact experiments were conducted to measure the stiffness and the transition of the contact force with the permission of the ethical committee. The biofidelity of the dummy was discussed based on the stiffness, maximum dynamic contact force, and the parameters of the viscoelastic model. The parameters were optimized using the genetic algorithm with MATLAB (with version 2019a) Simulink Model. The dummy is required for safety validation tests that involve injury from the viewpoint of the maximum dynamic contact force and the transferred energy.

In the future, we plan to change the target from the palm of the hand to the back of the hand. Another challenge is individuality - there is a wide variety of physical characteristics that are applicable for humans. By appropriately determining the mechanical properties, we can reproduce a worst-case scenario using the dummy.

Acknowledgment

This paper was financially supported by "Knowledge Hub Aichi" research project: R7 and conducted through "Construction of Risk Assessment System for Service Robot Applications: Establishment of A V&V Testing Method."

We would like to thank the Tanac Corporation for useful discussion and assistance with many samples.

References

[1] K. Suita, Y. Yamada, N. Tsuchida, K. Imai, H. Ikeda, and N. Sugimoto, "A failure-to-safety" Kyozon" system with simple contact detection and stop capabilities for safe human-autonomous robot coexistence," *Proceedings of 1995 IEEE International Conference on Robotics and Automation*, vol. 3, pp. 3089–3096, 1995.

[2] Y. Yamada, K. Suita, K. Imai, H. Ikeda, and N. Sugimoto, "A failure-to-safety robot system for human-robot coexistence," *Robotics and Autonomous systems*, vol. 18, no. 1-2, pp. 283–291, 1996.

[3] Y. Yamada, Y. Hirasawa, S. Huang, Y. Umetani, and K. Suita, "Human-robot contact in the safeguarding space," *IEEE/ASME transactions on mechatronics*, vol. 2, no. 4, pp. 230–236, 1997.

[4] T. Saito and H. Ikeda, "Measurement of human pain tolerance to mechanical stimulus of human-collaborative robots," *Specific Research Reports of the National Institute of Industrial Safety (NIIS-SRR)*, vol. 33, pp. 15–23, 2005 (in Japanese).

[5] B. Povse, D. Koritnik, T. Bajd, and M. Munih, "Correlation between impact-energy density and pain intensity during robot-man collision," *2010 3rd IEEE RAS & EMBS International Conference on Biomedical Robotics and Biomechatronics*, pp. 179–183, 2010.

[6] ISO/TS 15066: Robots and robotic devices-collaborative robots, 2016.

[7] T. Pilz, "Of the necessity of a uniform measurement procedure for the determination if the threshold values listed in ISO TS 15066," *9th International Conference on Safety of Industrial Automated Systems*, p. 48, 2018.

[8] Code of Federal Regulations Title 49, Chapter V - National Highway Traffic Safety Administration, Department of Transportation, Part 572: Anthropomorphic Test Device, 2011.

[9] S. Haddadin, A. Albu-Schaffer, and G. Hirzinger, "The role of the robot mass and velocity in physical human-robot interaction-Part I: Non-constrained blunt impacts," *2008 IEEE International Conference on Robotics and Automation*, pp. 1331–1338, 2008.

[10] Y. Shimaoka, T. Okamoto, and R. Watanabe, "Contact Area Effects on Superficial and Deep Pain Threshold for Service Robot Safety Design using a Pain-sensing System: Development of a Human-inspired Pain-sensing System (Special Issue B2B Solution)," *Panasonic technical journal*, vol. 65, no. 1, pp. 21–26, 2019 (in Japanese).

[11] G. T. Desmoulin and G. S. Anderson, "Method to investigate contusion mechanics in living humans," *Journal of forensic biomechanics*, vol. 2, 2011.

[12] T. Fujikawa, R. Sugiura, R. Nishikata, and T. Nishimoto, "Critical contact pressure and transferred energy for soft tissue injury by blunt impact in human-robot interaction," *2017 17th International Conference on Control, Automation and Systems (ICCAS)*, pp. 867–872, 2017.

[13] R. Sugiura, T. Fujikawa, R. Nishikata, and T. Nishimoto, "Soft tissue bruise injury by blunt impact in human-robot interaction-difference of tolerance between chest and extremities," *2019 19th International Conference on Control, Automation and Systems (ICCAS)*, pp. 792–797, 2019.

[14] DGUV: Collaborative robot systems - Design of systems with "Power and Force Limiting Function" function. Technical Report FB HM-080 Issue 08/2017, Deutsche Gesetzliche Unfallversicherung, 2017.

[15] B. Povse, D. Koritnik, R. Kamnik, T. Bajd, and M. Munih, "Industrial robot and human operator collision," *2010 IEEE International Conference on Systems, Man and Cybernetics*, pp. 2663–2668, 2010.

[16] U. Dinnar, "A note on the theory of deformation in compressed skin tissues," *Mathematical Biosciences*, vol. 8, no. 1-2, pp. 71–82, 1970.

[17] C. Pailler-Mattei, S. Bec, and H. Zahouani, "In vivo measurements of the elastic mechanical properties of human skin by indentation tests," *Medical engineering & physics*, vol. 30, no. 5, pp. 599–606, 2008.

[18] F. Khatyr, C. Imberdis, P. Vescovo, D. Varchon, and J.-M. Lagarde, "Model of the viscoelastic behaviour of skin in vivo and study of anisotropy," *Skin research and technology*, vol. 10, no. 2, pp. 96–103, 2004.

[19] M. Abellan, J. Bergheau, and H. Zahouani, "Comparison of different viscoelastic models for the characterisation of mechanical properties of human skin in vivo by indentation test," *Comput. Meth. Biomech. Biomed. Eng*, vol. 17, pp. 22–23, 2014.

[20] A. Nava, E. Mazza, F. Kleinermann, N. J. Avis, and J. McClure, "Determination of the mechanical properties of soft human tissues through aspiration experiments," *International Conference on Medical Image Computing and Computer-Assisted Intervention*, pp. 222–229, 2003.

[21] X. Wang, J. A. Schoen, and M. E. Rentschler, "A quantitative comparison of soft tissue compressive viscoelastic model accuracy," *Journal of the mechanical behavior of biomedical materials*, vol. 20, pp. 126–136, 2013.

[22] H. Shin, S. Kim, K. Seo, and S. Rhim, "A real-time human-robot collision safety evaluation method for collaborative robot," *2019 Third IEEE International Conference on Robotic Computing (IRC)*, pp. 509–513, 2019.

[23] B. R. Vemula, M. Ramteen, G. Spampinato, and B. Fagerström, "Human-robot impact model: For safety assessment of collaborative robot design," *2017 IEEE International Symposium on Robotics and Intelligent Sensors (IRIS)*, pp. 236–242, 2017.

[24] J. Liu, "MATLAB simulation of advanced PID control," *Beijing: Publishing house of electronics industry*, 2004 (in Chinese).